JOURNAL OF MATERIALS SCIENCE 28 (1993) 5875–5879

# Phase-transition toughening of high-$T_c$ superconducting ceramics

G. G. SIU
*Department of Physics and Material Science, City Polytechnic of Hong Kong, Hong Kong*
W. G. ZENG
*2302, Dongguan, Institute of Technology, Guangdong 511700, People's Republic of China*

The effect of the superconducting transition (SCT) on the plane-strain fracture toughness $K_{1c}$ of YBCO and BSCCO is studied by the method of three-point bend loading at room temperature and at 77 K. Toughening is observed and related to variation of the Gibbs free energy through the SCT, and hence to the condensation energy of a Cooper-pair gas. This is explained by the additional energy needed to excite superconducting electrons to normal ones in crack surfaces owing to magnetic field penetration. The superconducting gap parameters of YBCO and BSCCO are estimated and the results are reasonable.

## 1. Introduction

Mechanical properties of superconductor (SCs) such as elasticity, bending strength, hardness and toughness are of vital importance if SCs are to be applied as engineering materials. Extensive studies on SC mechanical properties have been carried out for both classical and high-$T_c$ SCs. These studies mainly follow a material science approach, emphasizing the interrelations between structure, properties and processing. In high-$T_c$ SCs (HTSCs), studies of mechanical properties relate macroscopic properties either to microstructure and basic thermodynamic quantities such as density and porosity [1], or to the fabrication techniques [2, 3], with the goal of improving quality by appropriate methods in powder preparation, sintering techniques, metal doping etc. [4, 5]. On the other hand, direct studies of the effect of superconductivity on mechanical properties provide (vice versa) an understanding of the superconducting transition (SCT) [6–19].

The plane-strain fracture toughness $K_{1c}$ predicts the ability of a material to resist rupture and is measured according to test standards, e.g. ASTM E399-72 to 83. The $K_{1c}$ characteristics of ceramics have been extensively studied due to the fact that these show less plastic deformation and so conform to linear elasticity theory. The $K_{1c}$ enhancement through a phase transition is called phase-transition toughening, which even becomes a processing technique for functional ceramics. A theory of phase-transition toughening [20–22] has developed which relates the difference of $K_{1c}^2$ before and after a phase transition to the change of the Gibbs free energy density $\Delta G$. Let the pre- and post-transition toughness be $K_0$ and $K_c$, respectively (in the original form, they are the critical stress intensity factors which become $K_{1c}$ in mode I loading). We have

$$K_c^2 - K_0^2 = \frac{2rEVF}{1 - \nu^2} \quad (1)$$

$K_c$ and $K_0$ are in units of Pa $m^{1/2}$; $r$ is the granular size (of the order of micrometres), $E$ the Young's modulus, $\nu$ the Poisson's ratio, $V$ the pre-transition volume fraction of the constituents to undergo the phase transition, and $F$ the work density of the stress field inducing the phase transition [20]:

$$F = |\Delta G| - F_1$$

where $\Delta G$ strongly depends on temperature and $F_1$ is the strain energy associated with the fraction released in the process of phase transition and fracture, almost independent of temperature. Usually, $F_1$ is negligible compared with $|\Delta G|$. $|\Delta G|$ can hence be determined. This theory has been applied successfully to the ceramic $ZrO_2$ [21, 22]. It is expected that it is also applicable to the HTSC ceramics.

SCT brings about a change of the Gibbs free energy density given by

$$G_N(T, P, 0) - G_S(T, P, 0) = \frac{1}{2}g\Delta^2 \quad (2)$$

where N is for the normal phase, S for the SC phase and 0 for zero magnetic field; $g$ is the energy-state density per unit volume at the Fermi surface and $\Delta$ the superconducting gap. Based on standard superconductivity theory, the SCT concerns the Bose–Einstein condensation of a gas of Cooper pairs (see e.g. [23]). The Gibbs free energy difference is directly related to the condensation energy rather than to an integral of negative magnetization $M$ over a range 0 to $H_c$ (the type I SC) or to $H_{c2}$ (type II), since for an HTSC its superconducting state with magnetic flux excluded is not a true thermodynamic equilibrium state (its magnetization curves are irreversible) and the integral of $-M$ has no definite physical meaning. The change of the Gibbs free energy could lead to toughening.

In this work we study two HTSC cuprate ceramics $YBa_2Cu_3O_x$ (YBCO) and $BiSrCaCu_2O_y$ (BSCCO).

0022–2461 

YBCO usually completes the structure transition from tetragonal to orthorhombic lattice [15] at a temperature above 700 K. So does BSCCO but it is, depending on sintering techniques, still a multi-phase system below 77 K [24]. Temperature reduction from 298 to 77 K does not cause other structural changes except a slight decrease of cell parameters and bond lengths [25]. For these materials the SCT is the only phase transition in the temperature region 77 to 300 K. The SCT should cause toughening as $\Delta G$ in Equation 2 is non-zero.

In this work the SCT effect on the fracture toughness $K_{1c}$ of YBCO and BSCCO is studied through measurements of three-point bend loading at room temperature and at 77 K. Phase-transition toughening through SCT is observed. The change of the Gibbs free energy determined from the toughening is related to the superconducting gap parameter. The estimated gap parameter is comparable to those obtained by other techniques.

## 2. Experimental procedure

### 2.1. Specimens

YBCO powder was prepared using the standard co-precipitation method from acetic acid solution of pure $Y_2O_3$ (99.99%), CuO (AR) and $BaCO_3$ (CP) in a predetermined ratio. The powder was compressed under 1.3 tonne $cm^{-2}$ pressure into rectangular pieces of approximate size 3 mm × 6 mm × 60 mm and sintered at 940 °C for 6 h. A second 6 h sintering was carried out after turning the sintered pieces upside down, with subsequent cooling to room temperature in the oven. Four-terminal resistivity measurements were then carried out to determine that the zero-resistance temperature $T_c$ (0) for each specimen was in the region 79–85 K. The resistive behaviour was metallic and diamagnetism appeared at 77 K (Fig. 1a).

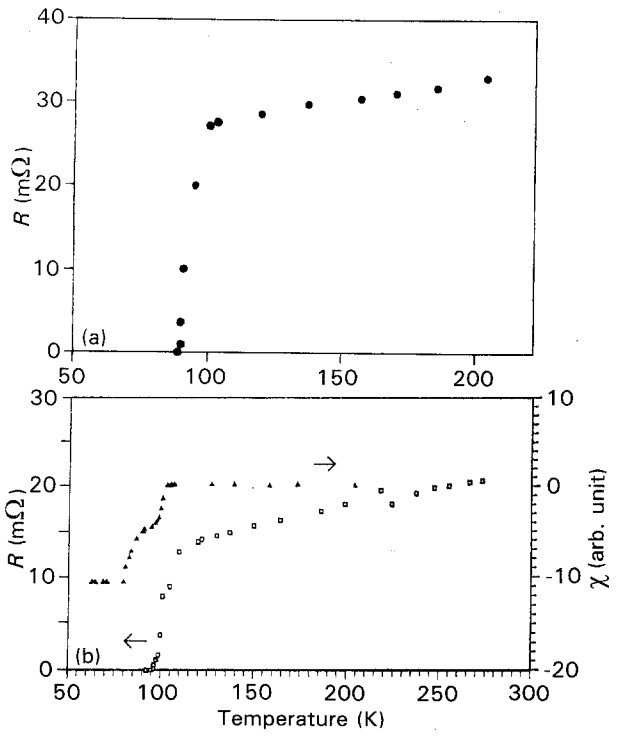


*Figure 1* Characterization of HTSC ceramics: (a) resistance versus temperature curve of a YBCO sample, (b) (□) resistance and (▲) magnetic susceptibility versus temperature of a BSCCO sample.

$Pb_{0.2}Bi_{0.8}SrCaCu_2O_y$ (BSCCO) was prepared using the solid-state reaction method from a mixture of PbO (CP), $Bi_2O_3$ (CP), $SrCO_3$ (AR), $CaCO_3$ (AR) and CuO (AR) in a predetermined ratio, preheated at 820 °C for 3 h (Pb and Bi were in 10 wt % excess to compensate for heating loss. Pb is not required in the original definition of BSCCO, which will be explained in the next paragraph). The powder was compressed under 1.3 tonne $cm^{-2}$ pressure into pieces of size 3 mm × 6 mm × 60 mm and sintered at 840 °C for 48 h. For these specimens $T_c$ (0) was in the region 85–90.5 K, their resistive behaviour was metal-like and they possessed partial diamagnetism (Fig. 1b).

The densities were 5.7 and 3.7 g $cm^{-3}$ for YBCO and BSCCO, respectively. The average grain size was 7 μm for both SCs based on measurements by an image analyser of SEM photographs. Standard characterizations such as structural identification using X-ray diffraction and $T_c$ determination using the four-probe technique essentially followed our previous works (see e.g. Fig. 1 in [15] and Fig. 5 in [19]). The YBCO sample was single-phase and BSCCO multi-phase. In fact, the partial substitution of Pb for Bi in the BSCCO system was aimed at raising the volume fraction of the 110 $K$-$T_c$ phase ($Bi_2Sr_2Ca_2Cu_3O_{10}$). Since the SCT is the only phase transition for BSCCO between room temperature and 77 K, its multi-phase character would not affect our interpretation of the experimental results.

Each specimen was cut into two for separate measurements at 300 and 77 K, respectively. After polishing, the size was 2.8 mm × 5.6 mm × 22.4 mm. A lengthwise notch was cut in the middle of one surface of each specimen by using a molybdenum wire of 80 μm diameter dipped in a mixture of emery and silicone oil. Each notch had a curvature radius $\rho = 55$–$60$ μm and a depth $a = 1.5$–$2.2$ mm, determined by a tool microscope of 3 μm resolution.

### 2.2. Fracture experiments

The fracture experiments were performed in a home-made small-size three-point-bend loading device, in which the radii of indenter and supports (made of smooth ceramic bars) were proportionately reduced according to the ASTM E399-83 test standard for plane-strain fracture toughness. The load $P$ was measured by a stress transducer with dynamometer calibration. The indenter displacement $\Delta'$ was measured using a micro-displacement transducer. Four-terminal resistance measurements, with silver colloid as the ohmic contact, were used to investigate the variation of resistance with pressure. A micro-ammeter was used to monitor the steady current at a value of 1.9 mA and voltage signals were taken across the notch. The $P$–$\Delta'$ and $R$–$\Delta'$ curves were recorded simultaneously. The resolution of resistance measurement was 8 and 5 μV $cm^{-1}$ for YBCO and BSCCO, respectively. The loading speed was 0.74 N $s^{-1}$. Experiments were carried out without magnetic shielding.

At 77 K all parts contacting the specimen were submerged in liquid nitrogen and loading started when the system temperature stabilized. After obtaining $P$–$\Delta'$ and $R$–$\Delta'$ curves, the notch depth $a$ and the curvature radius $\rho$ were checked by the tool microscope. According to the ASTM E399-83 test standard, the critical stress intensity factor $K_{1q}$ is determined from the fracture loading $P_q$ and geometric parameters including the notch depth $a$, sample thickness $B$, width $W$ and span $S$. The fracture surface was kept clean for further SEM analyses including energy spectrum analysis to check the average surface composition.

## 3. Results

The SEM studies of fracture surfaces show that flat breaks across crystallites dominate. Figs 2 and 3 show the $P$–$\Delta'$ and $R$–$\Delta'$ curves at 300 and 77 K, respectively. They all exhibit the characteristics of brittle fracture. Hence, the measured $K_{1q}$ is just the plane-strain fracture toughness $K_{1c}$. Table I lists the average values of $K_{1c}$ (each over six specimens) with the standard deviation, and the values of the three-point bend fracture intensity $\sigma_c = \frac{3}{2}P_qS/[B(W - a)^2]$ and the fracture surface energy $\Gamma = K_{1c}(1 - \nu^2)/2E$ resulting from linear elasticity theory, taking $\nu = 0.25$. Following Orange *et al.* [22], the curvature radius $\rho$ does not need correction in the range 55–60 μm. Despite the scatter in the toughness values caused by small variations of sample properties, the results confirm the enhancement of the fracture toughness of HTSC ceramics through the SCT. The measurement conditions and results are comparable to those previously reported (e.g. [3]) and they reproduce well.

Essentially, three points on the $K_{1c}$ versus $z(z = T/T_c)$ curve have been obtained, at $z \simeq 3$ ($T \simeq 300$ K), $z \gtrsim 1$ ($T_c < T = 77$ K) and $z \lesssim 1$ ($T_c > T = 77$ K). It is readily seen that $K_{1c}(z \lesssim 1) > K_{1c}(z \gtrsim 1) \simeq K_{1c}(z \simeq 3)$ from repetitive measurements on different samples. The original curves in Fig. 2 describe the behaviour of all samples at 300 K and the 77 K behaviour of the samples with $T_c(0) < 77$ K ($z > 1$). Fig. 3 represents the 77 K behaviour of those with $T_c(0) > 77$ K ($z < 1$). Hence, Fig. 2 is for samples in the normal state and Fig. 3 for those in the SC state. Inhomogeneity, impurities or BSCCO multi-phase character, of the porous granular ceramic samples have little influence in this macroscopic behaviour.

The electric conducting property was monitored by resistance measurements. In the normal state, the resistance of the specimen increases with pressure, as with ordinary materials. In the SC state, the zero-resistance is independent of the increase of pressure until the specimen is broken. This shows that at a resolution of 5–8 $\mu V\,cm^{-1}$, SC current exists all over the bulk SC specimen. In fracturing the number of SC current paths decreases, i.e. the critical current $I_c$ should reduce continuously, but the zero-resistance state of the sample holds as long as some SC paths still exist.

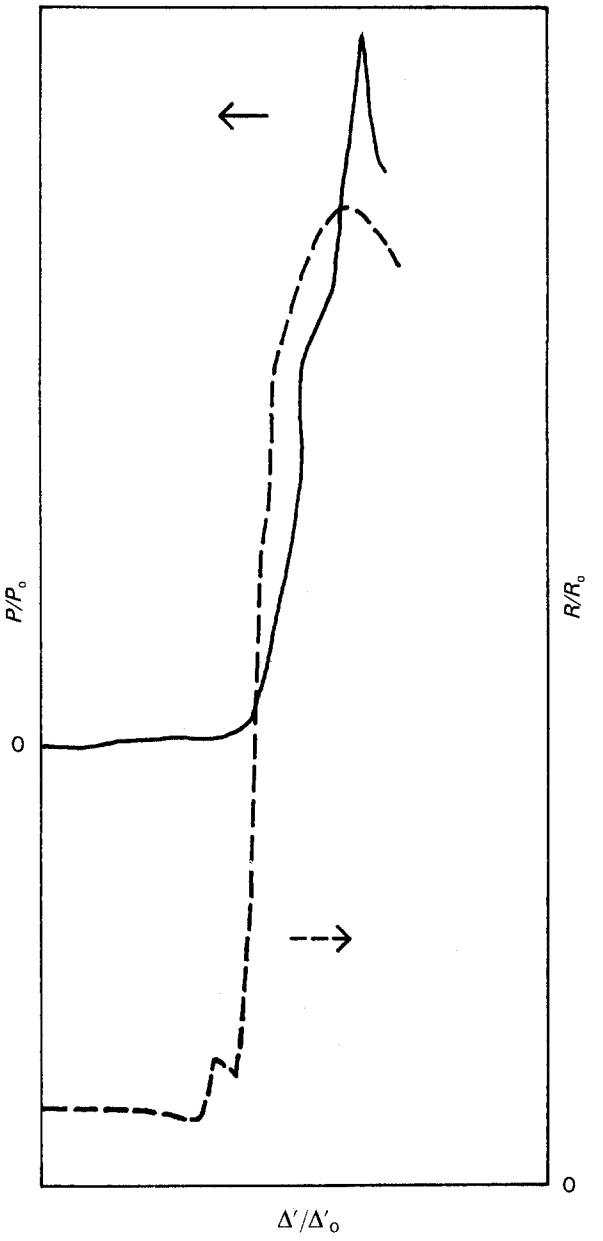


*Figure 2* Indenter-displacement dependence of three-point-bend loading $P$ and resistance $R$ for a YBCO specimen (similar for BSCCO sample) at 300 K (all in arbitrary units).

The order of magnitude of the compression elastic modulus $E$ was obtained from the compression stress–strain curve measured from the broken specimens. This was carried out by clamping each specimen between a steel indenter and a supporting steel plate. For YBCO specimens, the average $\langle E \rangle = 1.6 \times 10^5$ MPa and for BSCCO specimens $\langle E \rangle = 0.85 \times 10^5$ MPa. Energy spectrum analysis gave the compositions as follows: $YBa_{1.54}Cu_{2.12}O_x$ and $Pb_{0.17}Bi_{0.86}SrCa_{0.72}Cu_{1.26}O_y$.

From the experimental results, we conclude that the HTSC cuprate ceramics show phase-transition toughening through SCT.

## 4. Discussion

The plane-strain fracture toughness $K_{1c}$ of the HTSC ceramics was measured by conventional material science methods. The toughening is attributed to the

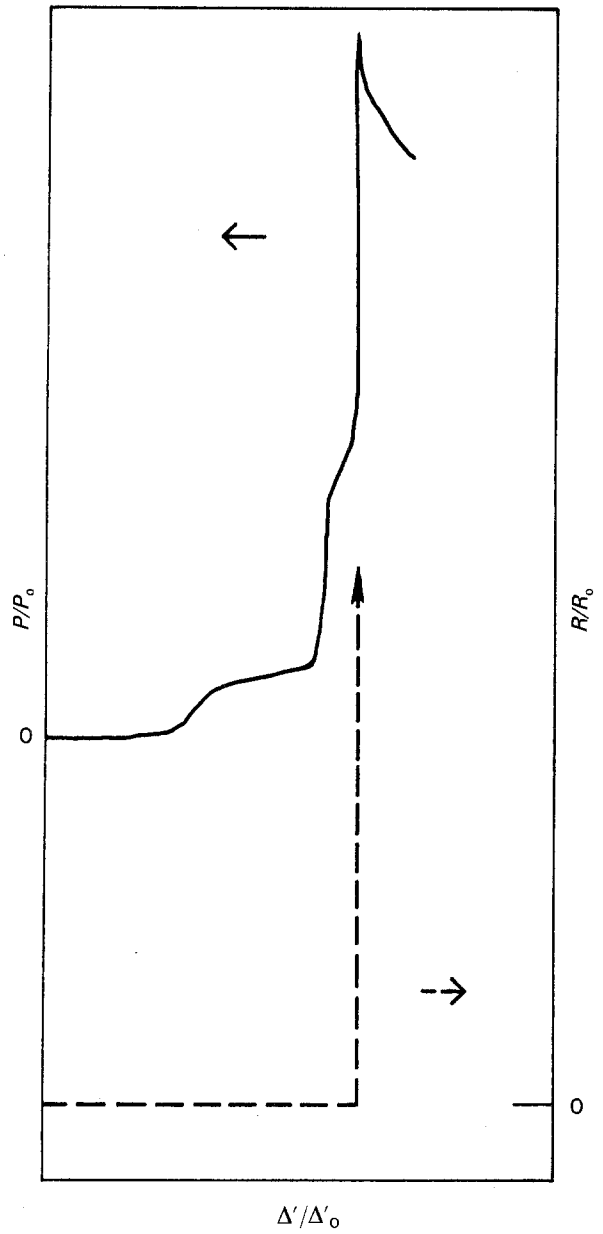


*Figure 3* Indenter-displacement dependence of three-point-bend loading $P$ and resistance $R$ for a YBCO specimen (similar for BSCCO sample) at 77 K (all in arbitrary units).

SCT and hence is associated with the condensation energy of a Cooper-pair gas. Before any physical information is extracted from the experiments, we have to substantiate this assumption by providing an interpretation.

In the process of brittle fracture of HTSC ceramics, strain energy is released for crack propagation, i.e. to provide the surface energy necessary for creation of the new surface. The energy for increasing a unit surface element of the crack is the fracture surface energy $\Gamma$. In the SC fracture, extra surface energy is needed owing to transformation of the interior superconducting state to the surface normal state in cracks by magnetic field penetration, resulting in enhancement of the fracture toughness. The depth of the normal-state surface is the thickness $\lambda$ of the penetration layer. A surface area increment $\Delta S$ results in excitation of condensed electrons to normal ones within a volume $\Delta S\lambda$, corresponding to additional energy $\frac{1}{2}g\Delta^2\Delta S\lambda$. Considering the volume fraction $V$ for ceramics, the increase of the fracture surface energy is

$$\Delta\Gamma = \frac{1}{2}g\Delta^2\lambda V \tag{3}$$

The fracture toughness is proportional to the fracture surface energy through

$$\Gamma = K_{1c}^2\frac{(1-\nu^2)}{2E}$$

We obtain

$$K_c^2 - K_0^2 = \tfrac{1}{2}g\Delta^2\frac{2\lambda EV}{1-\nu^2} \tag{4}$$

Equation 4 is similar to Equation 1 except that the penetration depth $\lambda$ replaces the granule size and the volume fraction $V$ is that of the superconducting constituents. It shows that our assumption is reasonable.

From Equation 4, the superconducting gap is

$$\Delta = \left((K_c^2 - K_0^2)\frac{1-\nu^2}{g\lambda EV}\right)^{1/2} \tag{5}$$

The three-point-bend loading is hence providing an estimate of the SC gap. We take the average $T_c = 82$ K and 87.8 K for YBCO and BSCCO samples, respectively. For granular porous superconducting ceramics, only an effective penetration depth of the polycrystalline sample is meaningful [26], which should be at least an order of magnitude larger than the penetration depth defined for a single crystal. YBCO single crystals have provided the most complete data [27] in the low-temperature limit: $\lambda_{ab} = 140$ nm and $\lambda_c \simeq 700$ nm and they rise precipitously when $T$ approaches $T_c$ [23]. It will be reasonable to estimate $\lambda_{eff}$(YBCO, 77 K; $T_c = 82$ K) $\simeq 40$ μm and $\lambda_{eff}$(BSCCO, 77 K; $T_c = 87.8$ K) $\simeq 20$ μm, values which are several times larger than the average granule size. By taking the values in Table I, rational values

TABLE I Average values of $K_{1c}$, $\sigma_c$ and $\Gamma$

| Sample | $T_c(0)$(K) | Test temperature (K) | $K_{1c}$(MPa m$^{1/2}$) | $\sigma_c$(MPa) | $2\Gamma$(J m$^{-2}$) |
|---|---|---|---|---|---|
| YBCO | 79–85 | 300 | 0.94 ± 0.12 | 27 | 5.1 |
| | | 77 | 1.21 ± 0.16 | 36 | 8.4 |
| BSCCO | 85–90.5 | 300 | 0.13 ± 0.03 | 3.6 | 0.19 |
| | | 77 | 0.25 ± 0.06 | 7.1 | 0.69 |
| BSCCO | < 77 | 300 | 0.15 ± 0.04 | 4.7 | 0.25 |
| | | 77 | 0.13 ± 0.03 | 4.0 | 0.19 |

$V = 0.7$ and 0.3 and carrier densities $n = 2.6$–$5.0$ and $2.2$–$4.6 \times 10^{21}\,\mathrm{cm}^{-3}$ [23, 25] for YBCO and BSCCO, respectively, and the Fermi energy $E_F = 0.4$ eV, we estimate (adopting the approximation $g/n \simeq 3/2E_F$)

$$\Delta(\mathrm{YBCO}) \simeq (1.3\text{–}1.7) k_B T_c$$

$$\Delta(\mathrm{BSCCO}) \simeq (1.0\text{–}1.5) k_B T_c.$$

These values are comparable to those from other studies: $2\Delta(0\,\mathrm{K}) = (5\text{–}8) k_B T_c$ [25], despite all the uncertainties concerning the microscopic parameters and the crudity of the approximations. These values also show the temperature dependence of the gap: $\Delta$ reduces in magnitude when $T$ approaches $T_c$. However, intrinsic uncertainties in our estimate and insufficient data hinder an affirmative conclusion. Nevertheless, this estimate shows that, qualitatively, the concept of phase-transition toughening may be applicable not only for a structural phase transition but also for SCT (second order).

## 5. Summary

The plane-strain fracture toughness $K_{1c}$ of HTSC cuprate specimens is in the range of 0.1–1.0 MPa $m^{1/2}$ and its values at 77 K are higher than those at 300 K. This is the phase-transition toughening of HTSC, and it can be explained by the additional energy needed to excite superconducting electrons to normal ones in crack surfaces owing to magnetic field penetration. The theory of phase-transition toughening for ordinary ceramics is hence applicable to HTSC with minute modification.


## Acknowledgement

This work is supported by the Indicated Research Grant of the City Polytechnic of Hong Kong and the Science and Technology Foundation of Guangtong Province, People's Republic of China.


## References


1. J. W. SERVERIN and G. de WITH, *Br. Ceram. Proc.* **40** (1988) 249.
2. J. E. BLENDELL, C. K. CHIANG, D. C. CRAMMER, S. W. FREIMAN, E. R. FULLER, E. DRESCHER-KRASICKA, W. L. JOHNSON, H. M. LEDBETTER, L. H. BENNETT, L. J. SWARTZENDRUBER, R. B. MARINENKO, R. L. MYKLEBUST, C. S. BRIGHT and D. E. NEWBURY, in "Chemistry of High-Temperature Superconductors", edited by D. L. Nelson, M. S. Whittingham and T. F. Gworge (American Chemical Society, Washington DC, 1987) p. 240.
3. N. McN. ALFORD, J. D. BIRCHALL, W. J. CLEGG, M. A. HARMER, K. KENDALL and D. H. JONES, *J. Mater. Sci.* **23** (1988) 761.
4. T. NISHIO, Y. ITOH, F. OGASAWARA, M. SUGANUMA, Y. YAMADA and U. MIZUTANI, *ibid.* **24** (1989) 3228.
5. Y. M. LIU, Y. Q. GAO, H. J. LIU, J. S. ZHOU, Y. F. WANG and W. H. SU, *Chinese Phys. (USA)* **10** (1990) 213.
6. L. C. BOURNE, A. ZETTL, K. F. CHANG, L. C. MARVIN, M. S. ANGELICA and W. K. HAM, *Phys. Rev.* **B 35** (1987) 8785.
7. D. J. BISHOP, P. L. GAMMEL, A. P. RAMIREZ, R. J. CAVA, B. BATLOGG and E. A. RIETMAN, *ibid.* **35** (1987) 8788.
8. D. J. BISHOP, A. P. RAMIREZ, P. L. GAMMEL, B. BATLOGG, E. A. RIETMAN, R. J. CAVA and A. J. MILLIS, *ibid.* **36** (1987) 2408.
9. H. MATHIAS, W. MOULTON, H. K. NG, K. K. PAN and R. J. KENNEDY, *ibid.* **36** (1987) 2411.
10. D. P. ALMOND, E. LAMBSON, G. A. SAUNDERS and WANG HONG, *J. Phys. F: Metal Phys.* **17** (1987) L221.
11. S. BHATTACHARYA, M. J. HIGGINS, D. C. JOHNSTON, A. J. JACOBSON, J. P. STOKES, J. T. LEWANDOWS and D. P. GESHORN, *Phys. Rev.* **B 37** (1988) 5901.
12. K. J. SUN, W. P. WINFREE, M. F. XU, K. SARMA BIMAL, M. LEVY, R. CATON and R. SELIM, *ibid.* **38** (1988) 11988.
13. H. MIZUBAYASHI, K. TAKITA and S. OKUDA, *ibid.* **37** (1988) 9777.
14. G. CANNELLI, R. CANTELLI, F. CORDERO, G. A. COSTA, M. FERRETTI and G. L. OLCESE, *ibid.* **36** (1987) 8907.
15. G. M. LIN, Q. Z. HUANG, J. X. ZHANG, G. G. SIU and M. J. STOKES, *Solid State Commun.* **68** (1988) 639.
16. W. G. ZENG, J. X. ZHANG, G. M. LIN, C. L. DU, P. C. W. FUNG and G. G. SIU, *ibid.* **70** (1989) 333.
17. W. G. ZENG, P. C. W. FUNG, G. M. LIN, J. X. ZHANG, G. G. SIU, Z. L. DU and K. F. LIANG, *ibid.* **71** (1989) 949.
18. J. X. ZHANG, G. M. LIN, W. G. ZENG, K. F. LIANG, Z. C. LIN, G. G. SIU, M. J. STOKES and P. C. W. FUNG, *Supercond. Sci. Technol.* **3** (1990) 113.
19. *Idem, ibid.* **3** (1990) 163.
20. F. F. LANGE, *J. Mater. Sci.* **17** (1982) 225.
21. A. G. EVANS, "Fracture in Ceramic Materials" (Noyes, Data Corporation US, 1985) p. 1.
22. G. ORANGE, G. FANTOGGI, Y. BIGAY and J. P. TORRE, *J. Physique C* **12** (1986) 655.
23. D. R. TILLEY and J. TILLEY, "Superfluid and Superconductor" (Hilger, Bristol, 1990) 38.
24. R. M. HAZEN, C. T. PREWITT, R. J. ANGEL., N. L. ROSS, L. W. FINGER, C. G. HADIDIACOS, D. R. VEBLEN, P. J. HEANEY, P. H. HOR, R. L. MENG, Y. Y. SUN, Y. Q. WANG, Y. Y. XUE, Z. J. HUANG, L. GAO, J. BECHTOLD and C. W. CHU, *Phys. Rev. Lett.* **12** (1988) 1174.
25. S. SATO, I. NAKADA, T. KOHARA and Y, ODA, *Acta Crystallogr. C* **44** (1988) 11.
26. J. RORENBLATT, *Rev. Physique Appl.* **9** (1974) 217.
27. B. BATLOGG, *Phys. Today* (June 1991) 44.
28. Z. X. ZHAO, in Proceedings of 3rd Asia Pacific Physics Conference, 20–24 June, 1988, Singapore, Vol. 1 (World Scientific, Singapore, 1988) p. 97.



*Received 6 July 1992*
*and accepted 27 April 1993*